Coupling analysis of heterogeneous integrated InP based photonic crystal triangular lattice band-edge lasers and silicon waveguides

Haroldo T. Hattori, Christian Seassal, Xavier Letartre, Pedro Rojo-Romeo, Jean L. Leclercq and Pierre Viktorovitch

LEOM-CNRS-Ecole Centrale de Lyon, 36 Avenue Guy de Collongue, 69134 Ecully France

Marc Zussy, Lea di Cioccio, Loubna El Melhaoui and Jean-Marc Fedeli

CEA-DRT/LETI 17 Rue des Martyrs 38054 Grenoble France
Christian.Seassal@ec-lyon.fr

Abstract: In recent years, many groups have envisioned the possibility of integrating optical and electronic devices in a single chip. In this paper, we study the integration of a photonic crystal laser fabricated in InP with a silicon passive waveguide. The coupling of energy between a 2D photonic crystal (PhC) triangular lattice band-edge laser and waveguide positioned underneath is analyzed in this paper. We show that a 40% coupling could be achieved provided the distance between the laser and the waveguide is carefully adjusted. A general description of the fabrication process used to realize these devices is also included in this paper.

OCIS codes: (130.0130) Integrated Optics, (140.2020) Diode Lasers, (220.4610) Optical fabrication

References and links

1. D. Liu and C. Svensson, "Power consumption estimation in CMOS VLSI circuit," IEEE J. Solid-State Circuits **29**, 663-670 (1994).
2. N. Savage, "Linking with light," IEEE Spectrum Online, Featured Article (2002).
3. S. Fan, P. R. Villeneuve, J. D. Joannopoulos, "Channel drop filters in photonic crystals," Opt. Express **3**, 4-11 (1998), http://www.opticsexpress.org/abstract.cfm?URI=OPEX-3-1-4.
4. T. Asano, M. Mochizuki, S. Noda, M. Okano, and M. Imada, "A channel drop filter using a single defect in a 2-D photonic crystal slab: defect engineering with respect to polarization mode and ratio of emissions from upper and lower sides," IEEE/OSA J. Lightwave Technol. **21**, 1370-1376 (2003).
5. T. Matsumoto and T. Baba, " Photonic crystal k-vector superprism," IEEE/OSA J. Lightwave Technol. **22**, 917-922 (2004).
6. S. Fan, S. G. Johnson, J. D. Joannopoulos, C. Manolatou, H. A. Haus, "Waveguide branches in photonic crystals," J. Opt. Soc. Am. B **18**, 162-165 (2001).
7. Y. G. Roh, S. Yoon, S. Kim, H. Jeon, S. H. Han, Q. H. Park, and I. Park," Photonic crystal waveguides with multiple 90° bends," Appl. Phys. Lett. **83**, 231-233 (2003).
8. J. Smajic, C. Hafner, D. Erni, "Design and optimization of an achromatic photonic crystal bend," Opt. Express **11**, 1378-1384 (2003), http://www.opticsexpress.org/abstract.cfm?URI=OPEX-11-12-1378
9. 0. Painter, R. K. Lee, A. Scherer, A. Yariv, J. D. O' Brien, P. D. Dapkus, and I. Kim, ″Two- dimensional photonic band-gap defect mode laser, ″ Science **284**, 1819-1821 (1999).
10. H. G. Park, J. K. Hwang, J. Huh, H. Y. Ryu, S. H. Kim, J. S. Kim, and Y. H. Lee, "Characteristics of modified single-defect two-dimensional photonic crystal lasers," IEEE J. Quantum Electronics **38**, 1353-1365 (2002).
11. C. Monat, C. Seassal, X. Letartre, P. Regreny, M. Gendry, P. Rojo-Romeo, and P. Viktorovitch, "Two-dimensional hexagonal-shaped microcavities formed in a two-dimensional photonic crystal on a InP membrane," J. Appl. Phys. **93,** 23-31 (2003).

#6909 - $15.00 US Received 18 March 2005; revised 15 April 2005; accepted 17 April 2005

12. H. Y. Ryu, M. Notomi, G. H. Kim, and Y. H. Lee, " High quality-factor whispering gallery mode in the photonic crystal hexagonal disk cavity," Opt. Express **12**, 1708-1719 (2004), http://www.opticsexpress.org/abstract.cfm?URI=OPEX-12-8-1708
13. K. Srinivasan, P. E. Barclay, O. Painter, J. Chen, A. Y. Cho, and C. Gmachl, "Experimental demonstration of a high quality factor photonic crystal microcavity," Appl. Phys. Lett. **83**, 1915-1917 (2003).
14. D. S. Song, S. H. Kim, H. G. Park, C. K. Kim, and Y. H. Lee, " Single-fundamental-mode photonic-crystal vertical-cavity surface-emitting lasers," Appl. Phys. Lett. **80**, 3901-3903 (2002).
15. N. Yokouchi, A. J. Danner, and K. D. Choquette,"Vertical-cavity surface-emitting laser operating with photonic crystal seven-point defect structure," Appl. Phys. Lett., **82**, 3608-3610 (2003).
16. H. T. Hattori, X. Letartre, C. Seassal, P. Rojo-Romeo, J. L. Leclercq, and P. Viktorovitch, "Analysis of hybrid photonic crystal vertical cavity surface emitting lasers," Opt. Express **11**, 1799-1808 (2003), http://www.opticsexpress.org/abstract.cfm?URI=OPEX-11-15-1799
17. D. Ohnishi, T. Okano, M. Imada, and S. Noda, "Room temperature continuous wave operation of a surface-emitting two-dimensional photonic crystal diode laser," Opt. Express **12**, 1562-1568 (2004), http://www.opticsexpress.org/abstract.cfm?URI=OPEX-12-8-1562
18. C. Monat, C. Seassal, X. Letartre, P. Viktorovitch, P. Regreny, M. Gendry, P. Rojo-Romeo, G. Hollinger, E. Jalaguier, S. Pocas, and B. Aspar, ″InP two-dimensional photonic crystal on silicon: In-plane Bloch mode laser,″ Appl. Phys. Lett. **81**, 5102-5104, (2002).
19. S. H. Kwon, H. Y. Ryu, G. H. Kim, and Y. H. Lee, ″Photonic bandedge lasers in two-dimensional square-lattice photonic crystal slab,″ Appl. Phys. Lett. **83**, 3870-3872 (2002).
20. S. Y. Lin, J. G. Fleming, and I. El-Kady, "Experimental observation of photonic-crystal emission near a photonic band edge," Appl. Phys. Lett. **83**, 593-595 (2003).
21. L. Florescu, K. Busch, and S. John, "Semiclassical theory of lasing in photonic crystals," J. Opt. Soc. Am. B **19**, 2215-2223 (2002).
22. J. Topol'ancik, S. Pradhan, P-C Yu, S. Gosh, and P. Bhattacharya, "Electrically injected photonic crystal edge-emitting quantum-dot laser source," IEEE Photon. Technol. Lett. **16**, 960-962 (2004).
23. S. G. Johnson, and J. Joannopoulos, "Bloch-iterative frequency domain methods for Maxwell's equations in a planewave basis," Opt. Express **8**, 173-190 (2001) http://www.opticsexpress.org/abstract.cfm?URI=OPEX-8-3-173
24. C. Monat, C. Seassal, X. Letartre, P. Regreny, P. Rojo-Romeo, P. Viktorovitch, M. Le Vassor d'Yerville, D. Cassagne, J.P. Albert, E. Jalaguier, S. Pocas, and B. Aspar, "Modal analysis and engineering of InP-based two-dimensional photonic crystal microlasers on a silicon wafer," IEEE J. Quantum Electron. **39**, 419-425 (2003)

1. Introduction

The increase of the integration density in microprocessors will lead to a technological bottleneck regarding interconnects in future years. More precisely, using the traditional metallic connections, power consumption will increase dramatically, and a lack of synchronism is expected in next generation chips [1]. One solution is provided by optical interconnects. Nowadays, optical connections are available to link different computers, but in the near future, optical interconnects may link different circuit boards. Moreover, it is expected that, in the future, optical interconnects will be able to make chip-to-chip communication and, eventually, connect subsystems on a chip. There are two basic approaches to realize this kind of optical interconnects: using free-space optics and optical waveguides. With the first approach, light is transmitted through air being focused by lenses and directed by diffraction gratings and mirrors. In the other approach, light is coupled into waveguides, where it is further directed to its destination. This last configuration is particularly attractive, notably because of the compactness of the resulting systems [2].

Among many possible ways to create such intrachip optical interconnects, our approach is illustrated in Fig. 1. It involves the integration of active devices (e.g. laser sources and photodetectors) made in III-V materials with electronic and passive optical components (waveguide, filters and routers), made in silicon. The optical signal should be in a wavelength range where there is no absorption in silicon, e.g. in the 1.3-1.55µm range. Therefore, InP and related alloys are preferred for the fabrication of the optoelectronics devices.

In this paper, we will focus on the sub-system constituted by the optical source and the passive waveguide. As device integration on the silicon chip should exhibit a small footprint,

#6909 - $15.00 US Received 18 March 2005; revised 15 April 2005; accepted 17 April 2005

we will only consider photonic structures that enable a very high confinement of photons. In our approach, the light source is a photonic crystal laser. Indeed, photonic crystals (periodic structures with high index contrast) allow the confinement of light in small volumes, and so lead to the fabrication of ultra-compact and relatively low threshold lasers. Moreover, fabrication of bi-dimensional (2D) PhCs is now well controlled and uses fabrication procedures very similar to those used to realize silicon integrated circuits. A multitude of devices has already been produced, such as filters [3-5], waveguide bends and branches [6-8], lasers [9-22], etc.

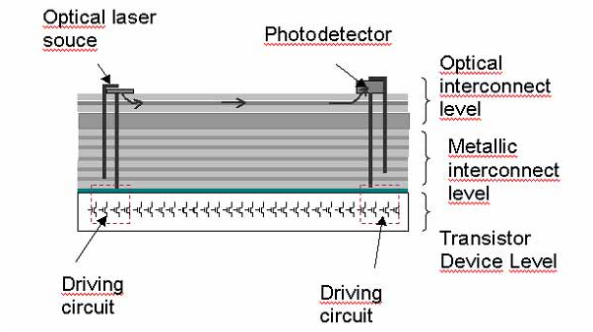

Fig. 1. A general scheme of a guided optical interconnect

Many laser configurations have already been analyzed in the literature, such as defect-mode [9-13], surface-emitting [14-17] and band-edge [18-21] lasers. The introduction of defects in a PhC lattice allows the design of high quality factor (Q) cavities [13], fact that may lead to the fabrication of low threshold laser devices. However, as mentioned by Ohnishi et al. [17], broad-area lasers such as band-edge lasers, have the advantage of providing larger output power, and better heat dissipation. Moreover, localized defects have a tendency to exhibit a radiation pattern with a weak directivity, what can make the coupling of the emitted light to waveguides more difficult.

Band-edge lasers, that operate at the edges of the first Brillouin zone (for example, the K or M point in a triangular lattice of air holes), can be considered as the photonic crystal equivalents of DFB lasers. In many cases, in these high symmetry points, a given mode exhibits extrema in its band diagram. At these extreme points, the group velocity can be made very small, meaning that the average lifetime of photons in the active area can be made large, significantly reducing the size of the device [18]. Moreover, as was argued by Florescu et al. [21], the fact that the group velocity of light is reduced near the band edges may provide an optical gain enhancement. If this high-symmetry point of operation is below the light line, we may expect that the chosen resonant mode in the PhC structure will be well confined in the vertical direction. Band-edge lasers in triangular [18] and square [19] lattices of air holes were analyzed recently. However, in those analysis, light was radiated in air. The goal of this paper is to analyze the coupling of light from the laser into a waveguide and, in the long-term, to use this sub-system in a complete optical link. At this stage we present simulation results and the fabrication scheme of this heterogeneous structure.

In this paper we restrict our attention to band-edge devices that consist of triangular lattices of air holes in a slab structure. The resonant mode in the PhC is assumed to be Transverse Electric (TE) (using the same convention as in [6]) and we consider the first mode in the valence band. The waveguide is single-mode both in the vertical and lateral directions (width of about 300 nm). No gain is introduced in the materials, since we are mainly concerned with the analysis of light coupling into waveguides, as shall be described in the text.

#6909 - $15.00 US Received 18 March 2005; revised 15 April 2005; accepted 17 April 2005

2. General analysis

The first structure to be analyzed is the one shown in Fig. 2(a) and 2(b). The PhC is a triangular lattice of air holes fabricated in the InP layer. Triangular lattice of air holes provide a larger bandgap than square lattice of air holes and that is the main reason for this choice. The InP layer has a thickness (h_1) of 250nm, while the thickness of the silicon waveguide (h_3) is chosen as 220 nm. With these two values of h_1 and h_3, the structures in the PhC and waveguide layers are single-mode in the vertical direction. Moreover, as h_1 is small, the evanescent field outside the InP and Si layers are more intense and they overlap quite efficiently. This allows a stronger coupling of light generated in the PhC laser into the waveguide. Here, it is assumed that the silica layer between the silicon wafer and the silicon waveguide is thick enough so that light leakage into the wafer is inhibited. The thickness of the intermediate layer (h_2) controls the coupling in the waveguide: if h_2 is too high, the coupling into the waveguide is very weak, if it is low, the coupling may be strong, but the optical losses induced in the PhC structure will be too high for lasing operation. More details about the choices of h_2, the Si waveguide width and the PhC parameters will be given in the text.

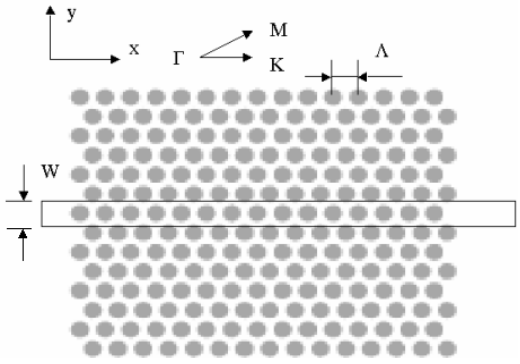

(a)

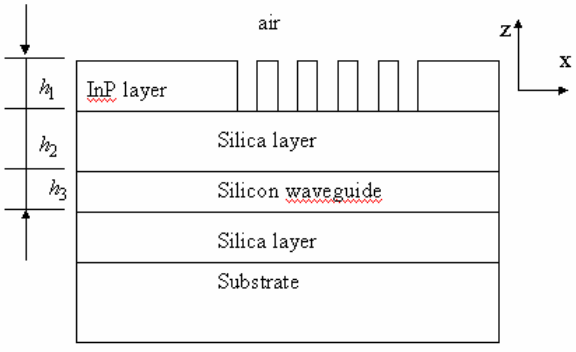

(b)

Fig. 2. (a). Z-cut view of the structure, showing a triangular lattice PhC and the waveguide situated in the bottom of the PhC. The waveguide is oriented in the ΓK direction (b) Vertical structure of the device, showing different layers. The silicon waveguide is surrounded (laterally) by a silica layer

The band diagram for the PhC structure, calculated by MIT's photonic bands software [23], is shown in Fig. 3 in the case of TE polarization and for a 47.5% filling factor (FF, ratio of the area occupied by the air holes in a primitive cell divided by the area of the primitive

#6909 - $15.00 US Received 18 March 2005; revised 15 April 2005; accepted 17 April 2005

cell). The normalized frequency is expressed in units of Λ/λ (Λ is the lattice parameter of the PhC and λ the free-space wavelength). In order to avoid diffractive coupling of light into silica and air, band edges that stand under the light line should be used. Namely, our devices based on a triangular PhC structure are assumed to operate at the K or M point of the first Brillouin zone. The lightline with respect to the silica layer is introduced in this band diagram as a dotted curve.

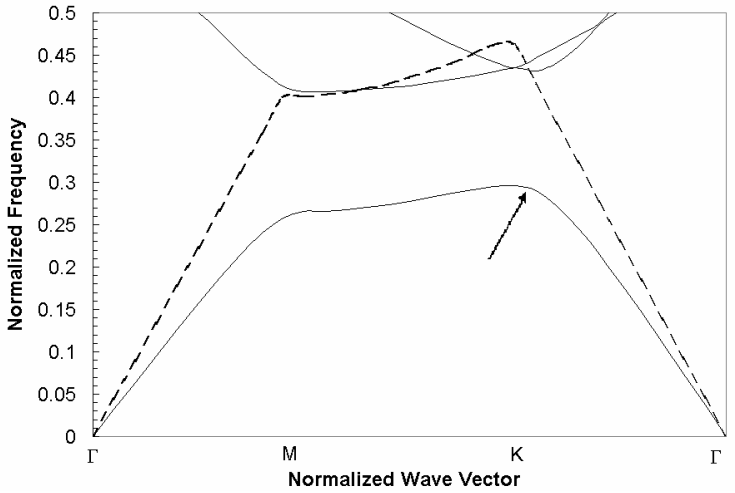

Fig. 3. Band diagram of the triangular lattice PhC structure

In order to perform an efficient optical coupling between the PhC resonant mode and the waveguide, it is necessary to have a good phase matching between the waveguide's propagation constant (β) and the wave vector along the considered direction of symmetry. The magnitude of the wave vectors along the ΓK and ΓM directions (at the first Brillouin zone, $\left|\vec{K}_{\Gamma K}\right|$ and $\left|\vec{K}_{\Gamma M}\right|$) can be expressed as,

$$\left|\vec{K}_{\Gamma K}\right| = \frac{4\pi}{3\Lambda} \tag{1}$$

$$\left|\vec{K}_{\Gamma M}\right| = \frac{2\pi}{\Lambda\sqrt{3}} \tag{2}$$

Having these parameters, we have to choose the operation point either at the K or M point, and the width (W) of the waveguide. If the K point is used, a 470 nm lattice constant should be chosen in order to operate close to λ= 1550 nm. For this lattice constant, the magnitude of the wave vectors along the ΓK directions is $\left|\vec{K}_{\Gamma K}\right| = 8.91x10^6$ rad/m. A simple effective index estimate shows that the propagation constant of the silicon waveguide is about $8.5x10^6$ rad/m, for W=300 nm. In that case, the phase matching to the PhC resonant mode along the ΓK direction is reasonable. If the M point is used, since $\left|\vec{K}_{\Gamma M}\right|$ is lower, phase matching can be achieved along the ΓM direction, but provided the waveguide width is reduced. This could be at the expense of additional propagation losses in the silicon waveguide. We finally chose to exploit the K-point of the first Brillouin zone (indicated with an arrow in Fig. 3).

#6909 - $15.00 US Received 18 March 2005; revised 15 April 2005; accepted 17 April 2005

Once the geometric parameters have been defined, the next step is to analyze the performance of the coupling of light from the PhC into a waveguide. Three-dimensional Finite-Difference Time-Domain (3D FDTD) method is used in the analysis. In these simulations, absorbing boundary conditions are placed at the edges of the computation volume. We have used a dipolar source to simulate the emission of quantum heterostructures [16]. The dipole is oriented in the y direction so as to generate light preferentially in the ΓK direction, and is positioned close to the middle of the PhC structure. Generally, a point detector is placed in the waveguide, and away from the area covered by the PhC region. If the simulation is launched without any waveguide (for reference purposes), the point detector is located in the InP layer, outside the PhC region.

For the basic structure shown in Fig. 2(a), with no waveguide, the spectrum detected outside the PhC region is shown in Fig. 4(a). It exhibits a series of peaks that correspond to the resonant modes of the PhC structure. In such spectra, the peaks are generally related to the fact that the lateral size of the PhC structure is limited. In particular, the peaks corresponding to the lowest values of the wavelength are cavity modes that are induced by the interaction between the low group velocity mode at the vicinity of the K point and the PhC edges. The peak that appears at λ=1534 nm corresponds to the fundamental cavity mode (indicated with an arrow in Fig. 4(a)). It exhibits the largest intrinsic quality factor (Q_i) of around 850. Now, if a waveguide is placed just underneath the structure (as shown in Fig. 2 (a) and (b)), additional optical losses will be induced and the quality factor of the chosen mode (Q_t) will be reduced. We assume that most of the extra losses are related to the evanescent coupling between the resonant and guided modes ; indeed, we are in the low coupling regime. With this assumption, the extra losses account for light coupling into the waveguide, and are represented by a quality factor Q_c , with:

$$\frac{1}{Q_t} = \frac{1}{Q_i} + \frac{1}{Q_c} \tag{3}$$

η_c , the estimated amount of power coupled into the waveguide with respect to the incident power, is then given by:

$$\eta_c = \frac{1/Q_c}{1/Q_i + 1/Q_c} \tag{4}$$

Therefore, we may consider this value of η_c as an upper bound of the actual coupling efficiency. Figures 4(b) and 4(c) respectively show the variation of Q_t and Q_c as function of h_2. One could note that the resonant wavelength changes only slightly with h_2. Figure 4(d) shows η_c as a function of h_2. On the basis of former experimental results [18, 24], with our setup and with our investigated materials, we expect the quality factor should be over 600 to observe laser emission. This yields h_2 > 700 nm and a maximum coupling efficiency of around 30%. Q factors well over 600 could be obtained by increasing h_2, in order to reduce the threshold of a laser based on such a PhC structure, but at the expense of a reduced coupling coefficient.

#6909 - $15.00 US Received 18 March 2005; revised 15 April 2005; accepted 17 April 2005

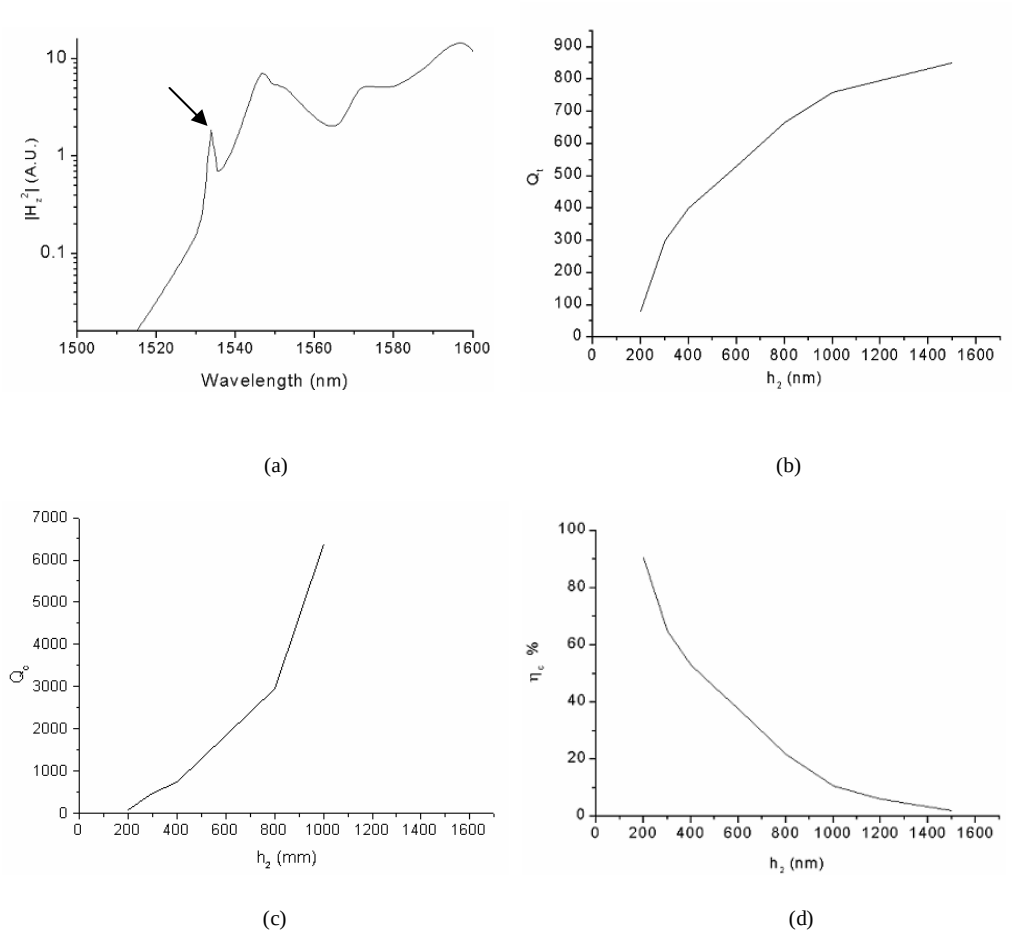

Fig. 4. (a). 3D FDTD spectrum of $|H_z^2|$ as a function of the wavelength for the basic structure with no waveguide (b) Total quality factor (measured in the waveguide) and (c) quality factor related to coupling losses as a function of h_2. (d) Coupling efficiency as a function of h_2. Results for the basic structure.

The field distributions for H_z in the structure are shown in Fig. 5(a) to 5(c), in the case h_2 = 600 nm. The PhC area is 6.58 μm (x-direction) by 5.66 μm (y-direction) and is centered in the computation area. Figure 5(a) shows a z-cut of H_z in the PhC region, at the main resonant peak, clearly showing the mapping of the fundamental mode. Part of the light escapes through the sides of the PhC structure (in the InP layer). Figure 5(b) shows that light is coupled into both directions of the waveguide underneath and that the mode is symmetric with respect to the x- axis. Figure 5(c) shows a y-cut of the structure and we can observe that light is significantly coupled into the waveguide.

#6909 - $15.00 US Received 18 March 2005; revised 15 April 2005; accepted 17 April 2005

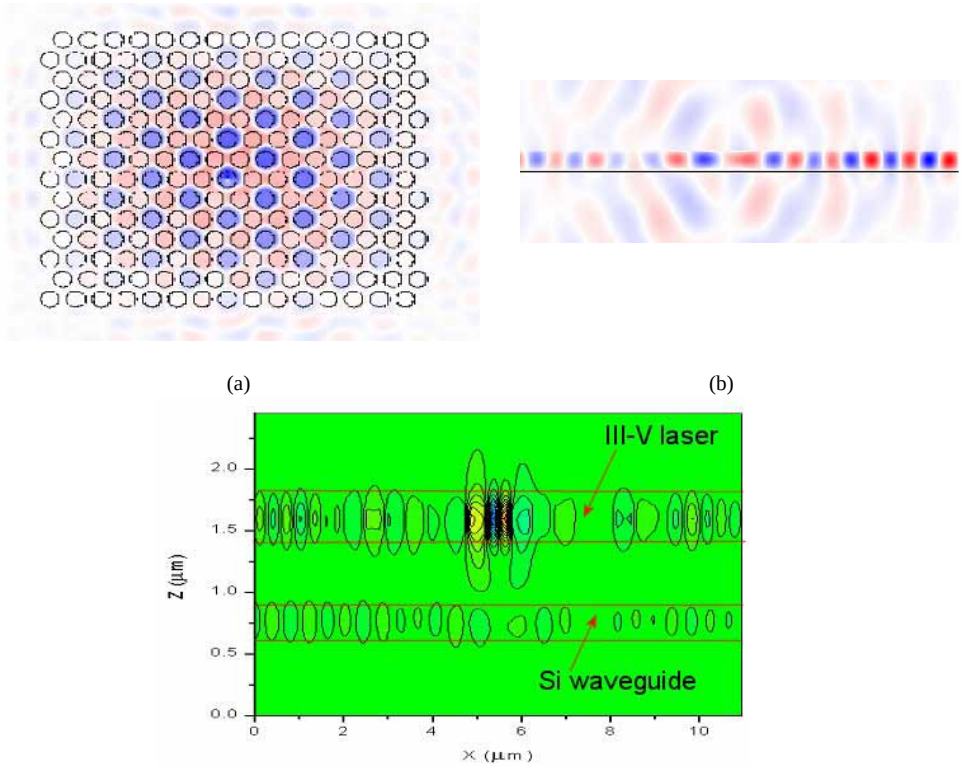

Fig. 5. (a). Field distribution (H_z component) in the PhC region (x-y plane). (b) H_z field distribution in the waveguide (x-y plane). (c) y-cut of the device, showing the field distribution of H_z. All these Fig. are for h_2=600 nm

From the results presented in Fig. 5, it appears that radiation losses in the vertical direction are low. However, a significant part of the light is lost (i) by coupling to the InP slab, beside the PhC area and (ii) because light is coupled to the waveguide into both directions, which is generally not relevant to the application. Then, one could imagine a more efficient design that select mainly one channel of optical losses. Following this view, we propose a more "directive" structure, schematized in Fig. 6(a). We have inserted a 1D grating in one side of the silicon waveguide, so that the coupled light can only travel in one direction. The grating has a lattice constant Λ_1 = 490 nm (constituted of alternating 270 nm long silica regions and 220 nm long silicon regions) and a width of 300 nm. Moreover, the main PhC, with a filling factor (FF) of 47.5 %, is surrounded, on three of its sides, by another PhC with FF=30% and same lattice constant, which acts as a shielding zone. This shielding PhC operates at its bandgap and the "shielding effect" improves with the number of rows.

The 3D FDTD spectrum for the situation where there is no bottom waveguide is shown in Fig. 6(b). Its main peak appears at λ= 1531.24 nm with a quality factor of 2000 (indicated with an arrow in Fig. 6(b)). Based upon the increase of the Q, it looks that the shielding has effectively reduced the lateral losses along three sides of the main PhC. On the other hand, more peaks appear in this spectrum, but the main peak is the one which exhibits the highest Q and also corresponds to the fundamental mode of the structure. The variation of Q_t, Q_c and η_c as a function of h_2 are shown respectively in Fig. 7(a), 7(b) and 7(c). In this second

#6909 - $15.00 US Received 18 March 2005; revised 15 April 2005; accepted 17 April 2005

design, the shielding increases the PhC resonant mode localization, and therefore, its k-vector distribution is larger. The consequence is that phase matching between the PhC resonator and the waveguide is worse ; finally, Q_c is higher than in the case of the first design. On the other hand, the shielding decreases the optical losses of the PhC resonator (Q_i). Finally, both Q_c and Q_t are increased, and η_c remains unchanged. In particular, to achieve laser emission in the PhC structure, we should have h_2 >300 nm. This leads to a coupling efficiency over 60%.

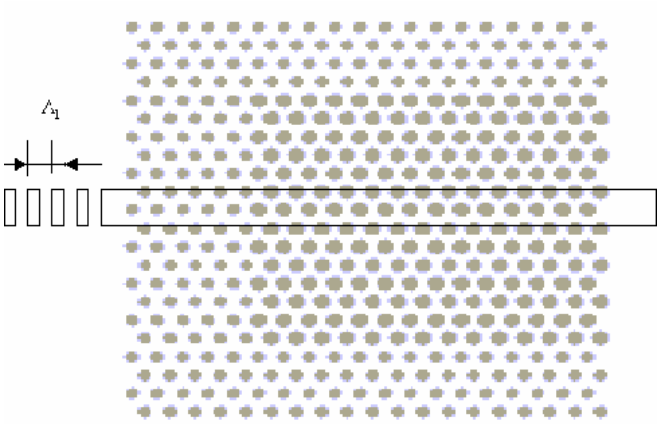

(a)

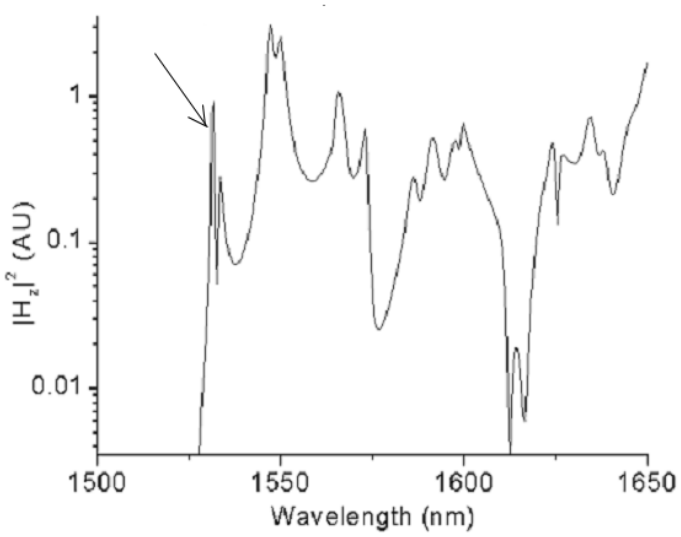

(b)

Fig. 6. (a). Z-cut view of the structure, showing the main PhC shielded by another triangular lattice PhC with lower FF (operating at its bandgap). The waveguide situated at the bottom of the structure has a 1D grating in one of his sides, also operating at the bandgap. (b) 3D FDTD spectrum of $|H_z{}^2|$ as a function of the wavelength for this structure with no waveguide.

#6909 - $15.00 US Received 18 March 2005; revised 15 April 2005; accepted 17 April 2005

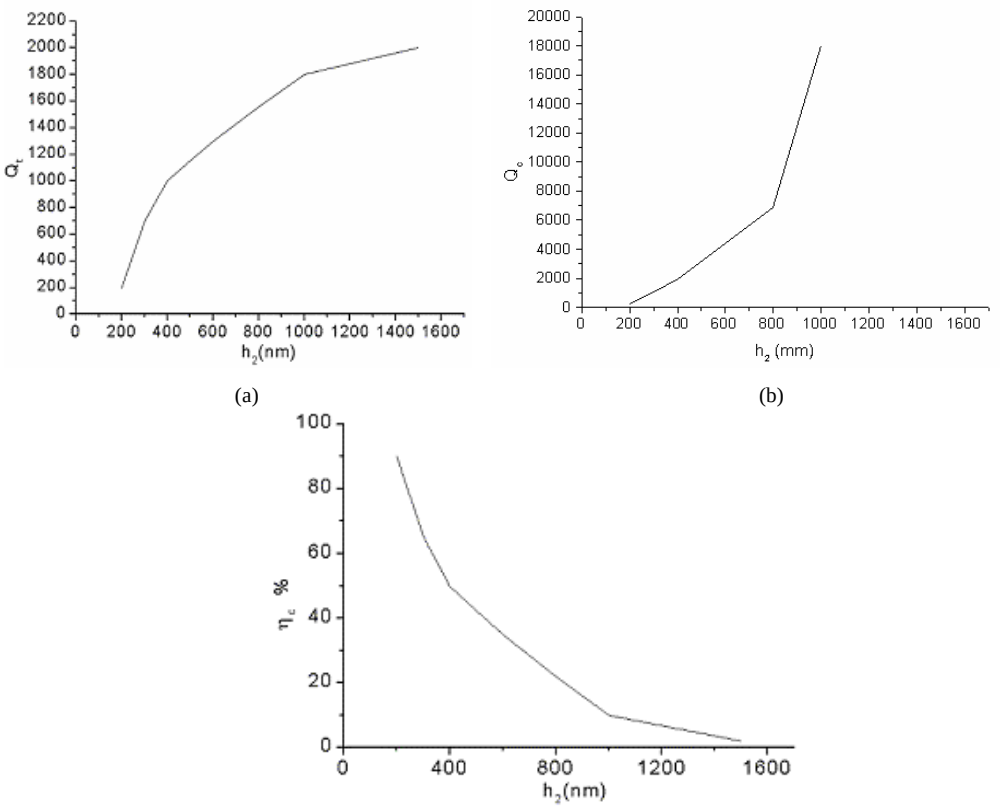

Fig. 7. (a). Total quality factor (measured in the waveguide) as a function of h_2. (b) Quality factor corresponding to coupling losses into the waveguide. (c) Coupling efficiency as a function of h_2. Results for the shielded structure.

Figure 8(a) shows the field distribution of $|H_z|$, at the main resonant peak, in the PhC region. It can be observed that the field is well confined in the PhC region and can only escape in the +x direction. Figure 8(b) shows the field distribution of $|H_z|$ in the waveguide. It can be clearly observed that the resonant mode is coupled to an even mode in the waveguide and that the coupling is quite directional. One could note that evanescent coupling into the waveguide is not highly localized ; therefore, the properties of the structure are not very sensitive to the position of the 1D grating. Figure 8(c) shows the field amplitudes of $|H_z|$ into the PhC and the waveguide, for h_2 =500 nm, showing that the coupling into the waveguide is efficient.

One could have expected a further increase of this beneficial effect by shielding all the borders of the PhC and not just three of them. However, in this case, the lateral losses into the membrane are inhibited, and the PhC resonator losses tend to be related to vertical scattering. The resonator would behave as a microcavity, and light localization would be much further increased. This would make the evanescent coupling between the PhC structure and the waveguide less efficient, and Q_c would be increased regardless of Q_i. This is the reason why we shielded just three sides of the PhC.

#6909 - $15.00 US Received 18 March 2005; revised 15 April 2005; accepted 17 April 2005

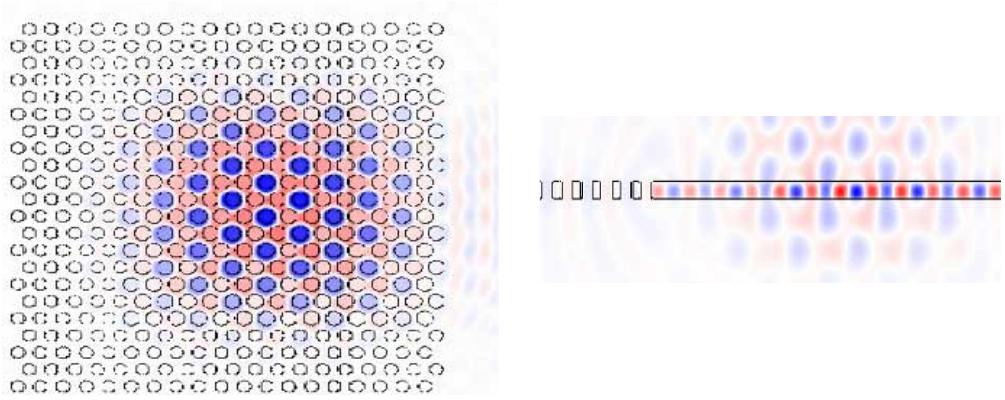

(a) (b)

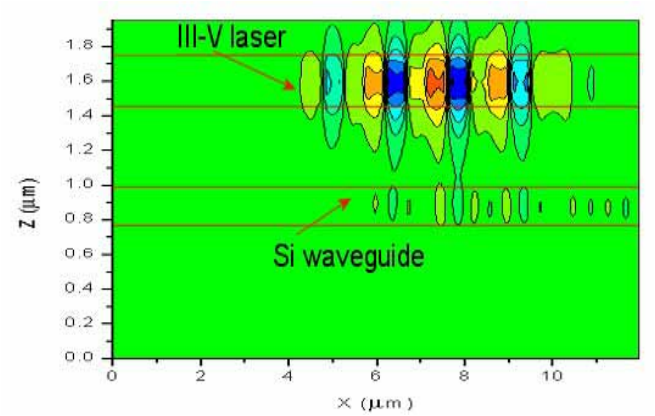

(c)

Fig. 8. (a). $|H_z|$ field distribution in the PhC region. (b) $|H_z|$ field distribution in the waveguide. (c) $|H_z|$ vertical field distribution in the x-z plane. All these Fig. are for h_2=500 nm.

3. Fabrication of the device

A specific process was developed to fabricate these heterogeneous III-V/silicon structures. The process flow is given in Fig. 9. The optical waveguide circuit is fabricated in a 200mm SOI (Silicon On Insulator) wafer that includes a 320 nm thick silicon layer on top of a 1μm thick buried oxide layer. Using this wafer, 0.3 to 1μm wide silicon wire waveguides are fabricated. For this study, electron beam lithography, hard mask, and reactive ion etching with HBr/Cl were used. Then, the passive photonic circuit is embedded in silica and planarised by CMP so as to obtain the proper thickness of silica above the guides. The active heterostructure has been grown by molecular beam epitaxy (MBE) on a 50mm InP wafer. This epilayer may contain an InAsP/InP quantum wells, designed to emit photons around 1.5μm. The total epilayer thickness is $\lambda/2n$, i.e. 240 nm in our case. A 10nm thin silica layer is then deposited by plasma-enhanced chemical vapor deposition assisted by electron cyclotron resonance (PECVD-ECR) on top of the active layer and the III-V wafer is then molecular bonded at the centre of the silicon wafer containing the photonic circuits. The final silica thickness between the passive silicon waveguides and the active layer (h_2) is the key parameter that controls the coupling coefficient between the laser mode and the guided mode.

#6909 - $15.00 US Received 18 March 2005; revised 15 April 2005; accepted 17 April 2005

After bonding, the InP wafer is chemically etched from the backside in HCl solution until the InGaAs etch-stop layer is reached, then this layer is selectively removed in a $FeCl_3$ solution. Electron beam lithography is used to pattern the PhC holes, with alignment accuracy better than ± 200nm. Finally, the PhC holes are transferred into the III-V heterostructure by reactive ion etching, using a CH_4:H_2 plasma. Figure 10 is a top view of a typical device including a PhC cavity and a Si wire waveguide underneath as a preliminary demonstration of the technological feasibility of these relatively complex and heterogeneous devices. This configuration might not be relevant with respect to optical coupling efficiency, but this example shows that the alignment between the Si waveguide and the PhC can be obtained with a good accuracy.

Next generation devices will be fabricated with optimized PhC structure and layer thicknesses, and should enable the experimental observation of the optical coupling between PhC laser and the silicon waveguides. Note that the design we propose is relatively tolerant, notably with respect to the SiO_2 bonding layer thickness. Indeed, if we consider a of ± 100 nm, the quality factor of the laser resonator is maintained in the 1000-1300 range, while the coupling efficiency is between 35% and 50 %.

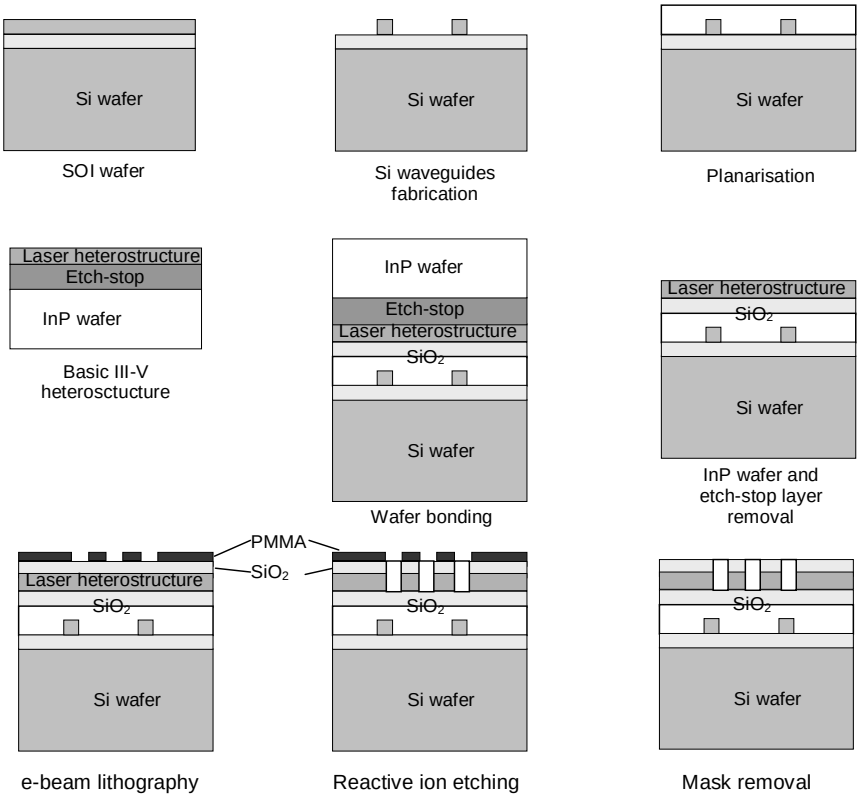

Fig. 9. Schematic description of the process steps used to fabricate PhC III-V microlaser on top of Si waveguides.

#6909 - $15.00 US Received 18 March 2005; revised 15 April 2005; accepted 17 April 2005

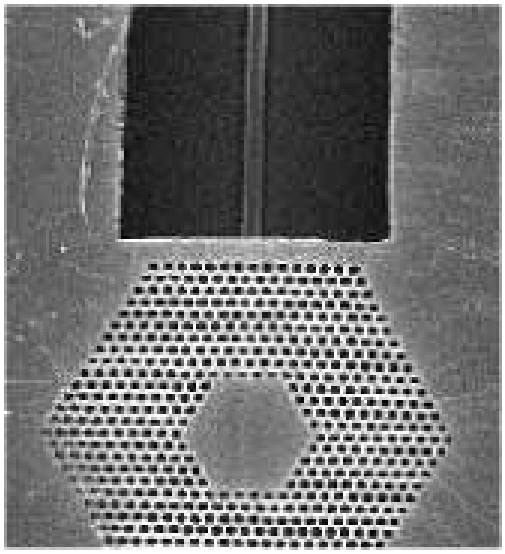

Fig. 10. SEM view of a III-V PhC micro-resonator (an hexagonal cavity) processed on top of a Si waveguide

4. Conclusions

We have analyzed III-V based photonic crystal band-edge lasers coupled to silicon waveguides positioned underneath. The initial basic structure could couple up to 30% of the incident power without sensibly degrading the lasing effect in the PhC region. By shielding three sides of the PhC, much higher coupling efficiency and directivity could be achieved, without degrading the properties of the PhC laser. For h_2 =300nm, the coupling efficiency is over 60%. Achievable fabrication tolerances on the thickness of the intermediate silica thickness of ± 100 nm, result in a coupling efficiency kept between 35% and 50 %, while the quality factor remains compatible with laser emission; this design is therefore robust to fabrication tolerances.

Acknowledgments

This work was supported by the European Union in the context of the European project FP6-2002-IST-1-002131-PICMOS.

#6909 - $15.00 US Received 18 March 2005; revised 15 April 2005; accepted 17 April 2005